Méthode multipolaire rapide des éléments de frontière appliquée aux problèmes de propagation acoustique en espace urbain

X. Vuylsteke[a], T. Leissing[b], P. Jean[a] et J.-F. Semblat[c]
[a]CSTB, 24 rue Joseph Fourier, 38400 Saint Martin D'Hères, France
[b]DCNS Research, Le Mourillon BP403, 83055 Toulon, France
[c]IFSTTAR, 14-20 Boulevard Newton Cité Descartes, F-77447 Marne La Vallée Cedex 2, France
xavier.vuylsteke@cstb.fr

For many years, the boundary elements method has been widely used to bring reference solutions for three dimensional outdoor propagation problems in homogeneous media. However, the BEM suffers a major drawback due to dense and unsymmetrical matrices. It may lead to prohibitive computation times, for a large number of degrees of freedom, making the BEM unusable at high frequencies or for large scale models. During the 80's, Greengard and Rokhlin introduced the Fast Multipole Method (FMM) to accelerate the matrix-vector product. Employed with the BEM, the FMM can reduce the prohibitive computation time through an iterative solver such as the Generalized Minimal RESidual (GMRES) method. First the theoritical formulation is synthetized. The scattering problem on a spherical body is then studied for mixed boundary conditions in order to prove the accuracy and the efficiency of the algorithm. Subsequently, we propose to deal with a half-space propagation problem before focusing on a more realistic configuration which could be encountered in urban acoustics.

1 Introduction

Based upon the Boundary Integral Equations (BIE) formulation, the Boundary Elements Method (BEM) [1] has emerged as a very promising numerical approach for solving exterior propagation problems. Due to the need to discretize the boundaries of the studied problem only, the BEM involves a 2 dimensional mesh for a 3 dimensional propagation problem. In addition, the boundary elements formalism satisfies the radiation condition at infinity which is suitable for infinite domain. However there are some drawbacks with the use of the BEM since the system of equation is dense, non-symmetrical and often ill-conditioned. As a result, solving a problem with the BEM requires $O(N^2)$ memory storage and also $O(N^3)$ operations, for N degree of freedoms, when direct solvers are used such as Gaussian elimination. Thus, dealing with large scale problems (hundreds of thousands elements) with the BEM results in a burden regarding the prohibitive computation times involved.

Since the 80's, the Fast Multipole Boundary Elements Method (FMBEM) has been widely studied to efficiently decrease the prohibitive computation time involved by the BEM. First reported by Greengard and Rokhlin [2] for the rapid evaluation of the potential fields governed by Laplace equation including a large number of particles, the Fast Multipole Method (FMM) has subsequently been extended to acoustical problems and Helmholtz equation [3] and elastodynamics [4, 5]. For a complete overview of the FMBEM and its application in physics, the reader can refer to [6]. Employed with an iterative solver such as the Generalized Minimum RESidual (GMRES) [7], FMBEM can efficiently reduce the computational cost to a linear dependence, $O(N)$. Even though common FMBEM use Wigner-3j symbol, the formalism developed by Gumerov et Duraiswami, based on the *direct Rotation - Coaxial translation - inverse Rotation* decomposition (RCR-decomposition), uses a set of coefficients which can be computed recursively [8]. It is this latter formalism which we have considered in the implementation of our FMBEM algorithm and which is reported in this paper. Furthermore, Rokhlin developed a high frequency formulation using a diagonal translation [9] and fast spherical transforms [10] to accelerate the translations for high frequencies. This formulation has subsequently led to a broadband/wide-band FMBEM algorithm including both low and high frequency formulations [11], [12].

The purpose of this paper is the application of a FMBEM algorithm to solve engineering problems of acoustic propagation in urban environments. First we present a general overview of the FMBEM formalism and introduce the mathematical backgrounds related to the BEM and FMBEM (section 2). Then, we compare the results obtained with our algorithm with analytical solutions of a scattering problem by a spherical body in order to prove its efficiency (section 3.1). Afterwards, we describe how ground reflections can be accounted for using the image source principle from a FMBEM point of view (section 3.2). Finally, our algorithm is assessed for a more realistic problem encountered in urban acoustics (section 4), a propagation problem in a quarter made of five buildings.

2 General overview and mathematical backgrounds

2.1 From the wave equation to the boundary integral equation

For three dimensional propagation in a homogeneous isotropic domain Ω, the wave equation in the frequency domain (i.e. the Helmholtz equation), can be written under the form:

$$\nabla^2\phi(\mathbf{x}) + k^2\phi(\mathbf{x}) = 0, \qquad \forall \mathbf{x} \in \Omega, \tag{1}$$

in which $\phi(\mathbf{x})$ is the acoustic pressure field at point $\mathbf{x}$, k is the wavenumber, ∇ is the nabla operator, $\nabla^2() = \partial^2()/\partial x^2 + \partial^2()/\partial y^2 + \partial^2()/\partial z^2$ for cartesian coordinates. Introducing the Green's function G as the free-space fundamental solution of the previous equation:

$$G(\mathbf{x},\mathbf{y}) = \frac{e^{ikr}}{4\pi r}, \quad \text{with} \quad r = |\mathbf{x}-\mathbf{y}| \quad \text{and} \quad i^2 = -1, \tag{2}$$

the Helmholtz equation (1) can now be rewritten under its boundary integral representation:

$$C(\mathbf{x})\phi(\mathbf{x}) = \int_S \left[G_k(\mathbf{x},\mathbf{y})q(\mathbf{y}) - \frac{\partial G_k(\mathbf{x},\mathbf{y})}{\partial \vec{n}_\mathbf{y}}\phi(\mathbf{y}) \right] dS_\mathbf{y} + \phi_{in}(\mathbf{x}), \tag{3}$$

where $\vec{n}_\mathbf{y}$ is the out-coming normal of the propagation domain Ω at the point $\mathbf{y}$ on the boundary S and $\phi(\mathbf{x})$, the incident wave at $\mathbf{x}$ from sources. The coefficient $C(\mathbf{x})$ is related to the fraction of local volume determined by the solid angle, γ, included in the domain Ω at point $\mathbf{x}$. The determination of the pressure field on the surface S, $\phi(\mathbf{x})$ requires to describe the Boundary Conditions (BC) on S. There are two typical types of problem in acoustic wave analysis referred as Dirichlet's and Neumann's problems:

$$\begin{aligned} &(\textit{Dirichlet BC}) \quad \phi(\mathbf{y}) = \bar{\phi}(\mathbf{y}), && \forall \mathbf{y} \in S, \\ &(\textit{Neumann BC}) \quad q(\mathbf{y}) = \frac{\partial \phi}{\partial \vec{n}} = \bar{q}(\mathbf{y}), && \forall \mathbf{y} \in S. \end{aligned} \tag{4}$$

We can also define a mixed (impedant or Robin's) conditions linking both previous quantities with the specific acoustic impedance Z:

$$\phi(\mathbf{y}) = Zq(\mathbf{y}), \qquad \forall \mathbf{y} \in S. \tag{5}$$

Equation (3) is also known as the Conventional Boundary Integral Equation (CBIE), allowing to determine ϕ at any point in Ω, once the values ϕ and q are known on the boundary.

2.2 Field representation by the fast multipole BEM

Since the FMBEM has been extensively covered in dedicated publications, we do not claim to do here a thorough description but rather a reminder of the method and the mathematical backgrounds used for the implementation. For a complete description of the fast multipole principle, we recommend to the reader Yijun Liu's book [6]. Furthermore, some details related to the *RCR-decomposition* method and the numerical aspects of its implementation can be found in Gumerov and Duraiswami's work [3].

The main idea of the Fast Multipole Method is the expansion of the fundamental solution of the Helmholtz equation on a spherical basis functions. We introduce a regular basis R and a singular basis S based upon a spherical harmonics series Y_n^m of degree n and order m, such as:

$$\begin{aligned} R_n^m(\vec{r}) &= j_n(kr)Y_n^m(\theta,\varphi), & S_n^m(\vec{r}) &= h_n(kr)Y_n^m(\theta,\varphi), \\ n &= 0,1,2,\ldots, & m &= -n,\ldots,+n, \end{aligned} \tag{6}$$

with the wavenumber k and the spherical coordinates (r,θ,φ). j_n and h_n denote the spherical Bessel functions and Hankel functions of the first kind, respectively. The Green's function (or the kernel G) in the BIE (3) can now be expanded in the following form:

$$G(\mathbf{x},\mathbf{y}) = ik\sum_{n=0}^{\infty}\sum_{m=-n}^{n} R_n^m(\mathbf{x}-\mathbf{x}^c)S_n^m(\mathbf{x}^c-\mathbf{y}^c)R_n^{-m}(\mathbf{y}-\mathbf{y}^c). \tag{7}$$

This expansion is theoretically an infinite sum of spherical basis functions performed between two points $\mathbf{x}$ and $\mathbf{y}$ and two intermediate points, the expansion centers $\mathbf{x}^c$ and $\mathbf{y}^c$ which fulfill the far field conditions:

$$|\mathbf{x}-\mathbf{x}^c| \ll |\mathbf{y}-\mathbf{x}^c| \quad \text{and} \quad |\mathbf{x}-\mathbf{y}^c| \gg |\mathbf{y}-\mathbf{y}^c|. \tag{8}$$

All points located in the area which do not respect this far field condition belong to the near field area and their contributions are taken into account using the straightforward formalism of the BIE. Consistent with the definitions (3) and (7), the Green's function derivative (or the kernel F) which appears in the BIE can also be expanded in 3 dimensions as:

$$F(\mathbf{x},\mathbf{y}) = ik\sum_{n=0}^{\infty}\sum_{m=-n}^{n} R_n^m(\mathbf{x}-\mathbf{x}^c)S_n^m(\mathbf{x}^c-\mathbf{y}^c)\frac{\partial R_n^{-m}(\mathbf{y}-\mathbf{y}^c)}{\partial \vec{n}_{\mathbf{y}}}, \tag{9}$$

which fulfill the far field criteria (8). Recurrence relations can be used for the computation of the basis functions as well as their derivatives. Precious information about the computational procedures can be found in the very detailed publication [8].

These expansions (eq. (7) and eq. (9)) allow the factorization of the potentials coming from the far field area leading to an acceleration of the matrix-vector product which appears in the iterative process of the solver. We can subsequently set up a hierarchical tree structure in order to group the potentials around the expansion centers and then perform the translations between these centers (cf. figure 1).

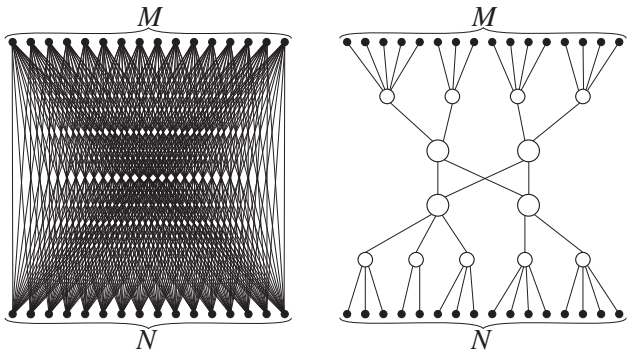

(a) straightforward method: number of operations $O(N \times M)$.

(b) Multi-Level FMM: number of operations $O(N + M)$.

Figure 1: *Comparison of the number of interactions between N sources and M receivers for (a) the BEM and (b) the fast multipole BEM. The lines show the interactions for each method, the filled circles symbolize the elements and the circles represent the expansion centers.*

2.3 Algorithm features

The FMBEM algorithm has been implemented in a Fortran 90 code. The purpose is to build a hierarchical tree consisting of several levels structured from the whole studied boundary. The computational domain is first embedded in a cube of vertice D, which is assigned to level 0, thereafter subdivided in an oct-tree structure from level 0 to level *lmax*. Since the FMBEM can handle a very large number of elements (several hundreds of thousands) on a desktop computer, the solution on the mesh is approached with constant elements (interpolation order 0), meaning that we only have one unknown at the center of each element. The algorithm includes both low and high frequencies formulations, according to the definition of Gumerov and Duraiswami in [12]. In order to translate the expansion coefficients from an expansion center towards another one, we use the translation method based on the *Direct rotation-Coaxial translation-Inverse rotation* (RCR-decomposition) introduced in [8] for the low frequency formulation in the low frequency levels (LF levels) and diagonal translation introduced by Rokhlin [9] for the high frequency formulation in the high frequency levels (HF levels). The iterative solver GMRES [7] is used to solve the matrix system. Therefore, for each iteration, only the matrix-vector product is stored and the whole matrix is never explicitly built.

3 Validation of the FMBEM algorithm with a scattering sphere problem

The purpose of this section is the validation of our FMBEM algorithm. We will focus, throughout this validation stage, on a spherical wave scattered by a spherical

body (see figure 2), for which an analytical solution exists, described in the following section. After detailing some useful parameters of our FMBEM algorithm, the analytical solution is taken as a reference solution to demonstrate the accuracy of the FMBEM for both rigid and mixed boundary conditions (section 3.1). The algorithm will be used subsequently as a reference to validate the half-space formalism, starting from its associated full-space problem, section 3.2

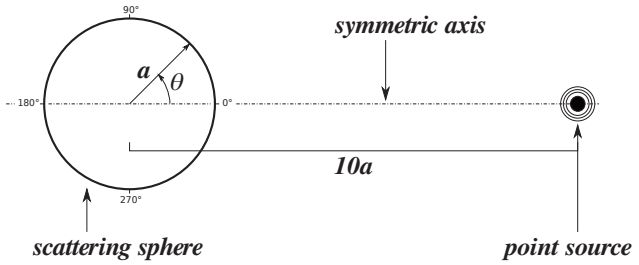

Figure 2: *Schematic of the studied problem: A sphere of radius a excited by a point source.*

3.1 Numerical study for a full-space propagation

Analytical solution We consider the case of a spherical body of radius a excited by a spherical wave generated by a point source of amplitude Q located at a distance $d = 10a$ from the sphere center. The acoustical surface potential $\phi|_S$ can be written as:

$$\phi|_S = -\frac{Q}{4\pi ka^2} \sum_{n=0}^{\infty} \frac{(2n+1)h_n(kd)P_n(cos\theta)}{h'_n(ka) + \sigma h_n(ka)}, \qquad (10)$$

where $\sigma = 1/Z$, is the complex admittance and θ, the azimuthal angle, is the angle between the radius vector of the surface point and the direction of the incident wave. We notice that this problem is axi-symmetric (see figure (2)) and is only depending on the variable θ, implying that only the solution for $\theta \in [0, \pi]$ needs to be computed to know the surface potential on the whole surface. Both equations bring into play Legendre polynomials $P_n(\mu)$ defined in the range $[-1, 1]$, spherical Hankel functions of the first kind h_n (often noted $h_n^{(1)}$) and their derivatives h'_n. Further information about the relations between Bessel's functions can be found in [13].

Algorithm parameters The validation tests are made for a sphere of radius a, whose surface is meshed with 31694 constant triangular elements. The maximum number of elements authorized at the lowest level is 50, which involves a tree consisting of 6 levels (4 useful levels). The level-dependent truncation number p, used for the expansion of kernels, is chosen to keep a very good accuracy. In order to validate the two formulations, we have performed several tests with both formulations: pure LF and HF tests in which only LF formalism or HF formalism are used. Considering the GMRES solver, we do not use a preconditioner and the stop criterion (the residual) is set to 1.10^{-3}. Since a small number of iterations is required in these validation procedures, the memory usage related to the Krylov subspace is small and we do not have to use the restart parameters (set to 200). All the computations are done on a desktop PC with an Intel Xeon® X5675 processor at 3.07 GHz and 12 GB storage memory.

Validation cases The analytical solution is taken as the reference solution for the verification of the FMBEM algorithm. We study the case of a spherical incident wave scattered by a spherical body with a radius a equal to 1 m (see figure 2). We compare the surface potential pressure level. The source, located at $10a$ from the sphere center, has a unit amplitude $Q = 1$ and the reference pressure chosen is $20\mu Pa$. 360 receivers are evenly distributed on the surface of the sphere. Figure 3 shows the comparisons of the sound pressure level in decibels, in terms of azimuthal angle in degrees, between the analytical solution (blue lines) and the solution computed with the FMBEM algorithm (dashed red lines). The comparison is performed for dimensionless wavenumbers: $ka = 0.1$ and 20, obtained for frequencies equal to 5.4 and 1082.4 Hz, respectively. In order to ensure that both kernels G and F are properly computed, we treat a rigid case ($q = 0$) for which only the computation of the kernel F is required, and also an impedant case for which both kernels G and F are required. The impedance has been chosen to study the limit cases of a rigid body (i.e. $\sigma = 0$), and a soft body with a normalized complex impedance (compared with the air) $Z/Z_A = \sigma_A/\sigma = 1.22 + 1.22i$.

We can see a very satisfactory consistency between both solutions (see figure 3), meaning that the FMBEM algorithm succeeds in working out the solution for the considered ka. Hence, the expansion of the kernel G (eq. 7) and its normal derivative F (eq. 9) on the spherical basis functions are relevant to keep a satisfactory accuracy.

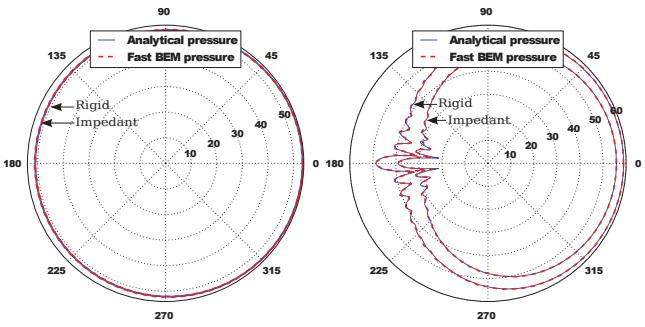

(a) $ka = 0.1$ (b) $ka = 20$

Figure 3: *Comparison between the analytical solution (blue lines) and the FMBEM solution (dashed red lines) of the sound pressure level in dB(SPL) on the surface of the sphere excited by a spherical source of unit amplitude $Q = 1$. The reference pressure is 20 μPa.*

3.2 Numerical study for a half-space propagation

The full-space acoustic problem studied in the previous section is actually unusable in urban acoustic. Indeed, due to the presence of the ground, the problems encountered in urban acoustic can be seen as semi-infinite problems. Thus dealing with a half-space problem can be solved either by meshing the geometry in the mirror domain or by taking into account the acoustic reflection on the ground thanks to a

fictitious rigid baffle. We will see in this section how to deal with a half-space problem in the framework of the FMBEM starting from its corresponding full-space problem. The half-space formalism introduced in this section is not an original work since it has already been the purpose of previous publications in two dimensions [14] and in three dimensions [15]. The problem of a whole rigid sphere, studied in the previous section corresponding to the full-space problem will be used as the reference solution. We will compare it to the half-space problem in which only a half-sphere, lying on a fictitious infinite rigid plane, needs to be meshed. The contributions of the image domain, which correspond to the ground reflections, will be added through the fictitious rigid baffle. The half-space problem is depicted in figure 4 and its corresponding full-space problem is depicted in figure 2.

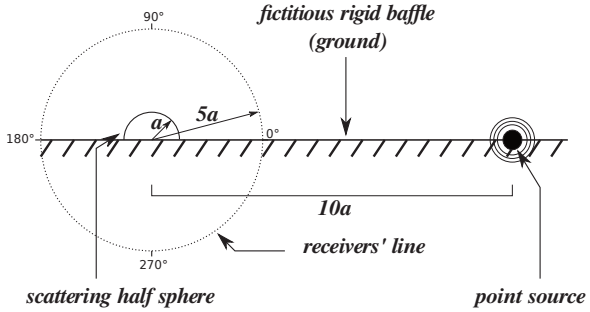

Figure 4: *Schematic of the validation case: A half sphere of radius a, excited by a point source .*

The half-space principle We present in this section the method to deal with a half-space problem starting from its associated full-space problem and we describe its implementation in the FMBEM algorithm. Since the urban ground can be considered in a first approach as a rigid plane, the implementation of the baffle is actually based upon the image source principle. As for the full-space problem, for each cell, the oct-tree structure is divided in two areas. The first area corresponds to the near elements and the second area corresponds to the far elements.

The contribution of the near elements is performed directly using the boundary integral equation. For each contribution from a near source element $\mathbf{x}$, towards a receiver element $\mathbf{y}$, we add the contribution coming from the image source element $\mathbf{x}'$ and thus the free space solution G becomes:

$$G(\mathbf{x},\mathbf{y}) \equiv G(\mathbf{x},\mathbf{x}',\mathbf{y}) = \frac{e^{ikr}}{4\pi r} + \frac{e^{ikr'}}{4\pi r'}, \qquad (11)$$

with r and r' being the distance from $\mathbf{x}$ and $\mathbf{x}'$ to $\mathbf{y}$ respectively.

The contribution of the far elements is performed using the multipole method. Each time that a translation is made in the moment step or in the moment to moment (M2M) step in the real space, from an expansion center to another one, a symmetric translation is also made in the image domain (see [14, 15]). This involves two translation matrices, which will be added at the same expansion center in the moment to local (M2L) step. Afterwards, there is no distinction between these two translation matrices and the local to local (L2L) step and the final summation remain unchanged. The principle of the contribution of the far elements in the half-space problem, from a FMBEM point of view, is summarized in figure (5).

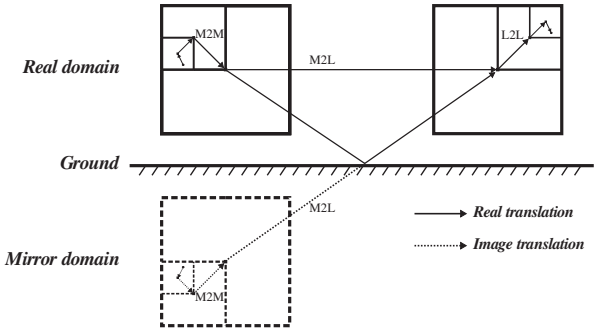

Figure 5: *General overview of a half-space problem: definition of the real and virtual objects by the FMBEM.*

Finally, for the calculation of acoustic pressure levels at the receivers away from the boundaries (in the post-processing step), the contribution coming from the ground is taken into account through the image source principle and added to the contribution of elements located in the real domain.

Numerical results We now compare the solution of the full-space with its corresponding half-space solution. For the half-space problem, we only have to mesh a half sphere involving two times less elements than for the full-space problem, 15846 (~31694/2) against 31694 elements respectively. Solutions are both computed with the FMBEM algorithm in order to only highlight the differences due to the rigid baffle. We compare the potential pressure level taken on 360 receivers, evenly distributed on a circle of radius $r = 5a$ from the sphere center. The computations are done for two frequencies, which correspond to the dimensionless wavenumber $ka = 0.1$ and 20.0. Note that we have halved the amplitude of the source for the half-space problem since it is taken into account twice, once in the real domain and also for the image domain. Figure 6 shows the potential pressure in dB taken on the receivers for the full-space problem (blue line) and for the half-space problem (red crosses).

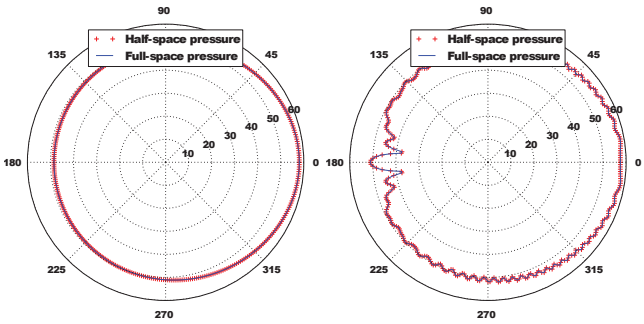

(a) $ka = 0.1$ (b) $ka = 20$

Figure 6: *Comparison between the full-space solution (blue line) and the half-space solution (red crosses) of the sound pressure level in dB(SPL) on a curved line of radius r = 5a. The reference pressure is 20 μPa.*

Since we cannot see significant differences (maximum discrepancy of 0.02 dB) between the full-space and the half-space solutions, the half-space problem with the addition

of the fictitious infinite rigid baffle is relevant to efficiently solve acoustic problems including the ground reflections without having to mesh the mirror object. We also notice that the half-space problem brings significant savings in terms of computation time and required memory mainly due to the fact that the half-space problem requires two times less number of elements than for its corresponding full-space problem.

4 Applications of the FMBEM to a propagation problem in a quarter

Since we have checked in the previous section both efficiency and accuracy of the half-space FMBEM for a spherical body, we now focus on a more realistic geometry, a large scale model in order to emphasize the benefits of the FMBEM as the number of elements increases.

This larger scale model represents a quarter, made of 5 buildings of 15 meters height and a total length of 110×60 meters. We performed the computation for a frequency range between 90 and 100 Hz with a 1 Hz step, involving 66306 elements at 100 Hz with a space discretization criterion of $\lambda/4$ (λ being the studied wavelength). The maximum number of elements allowed at the lowest level is 80, involving 5 useful levels. The mesh as well as the receivers' map is shown in figure 7. The point source is located at the coordinates $(12, 45, 0)$. For the sake of the high computation time involved by classical BEM, the comparison will be perform with an internal BEM software, *Micado3D* [16], which will be taken as a reference. It is an optimized 3 dimensional boundary elements algorithm based on a direct approach for the study of acoustical problems. It is based on a variational approach and uses linear interpolation functions.

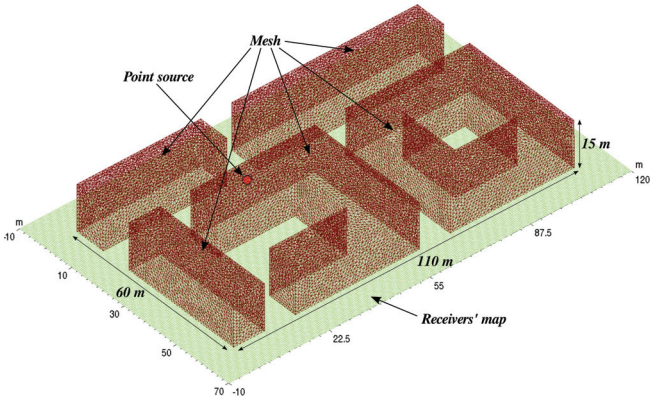

Figure 7: *overview of the studied geometry: A quarter made of 5 buildings (66306 elements, in red) excited by a point source and the receivers' map (41600 receivers, in green).*

Numerical results In figure 8 the sound pressure level in dB(SPL) calculated on the receivers' map (total length: 70 m $\times$ 130 m, i.e. $\sim 20\lambda \times \sim 40\lambda$) for both *Micado3D* and the FMBEM algorithms is displayed. These two maps seem to be in good agreement. At 100 Hz (for 66306 elements) the computation required around 8 hours on a Intel Xeon® E5645 processor at 2.40 GHz processor with the reference code *Micado3D* (optimized variational BEM) and about 20 minutes on an Intel Xeon® X5675 processor at 3.07 GHz for the FMBEM implementation. The details of computing resources required by both algorithms can be found in table 1.

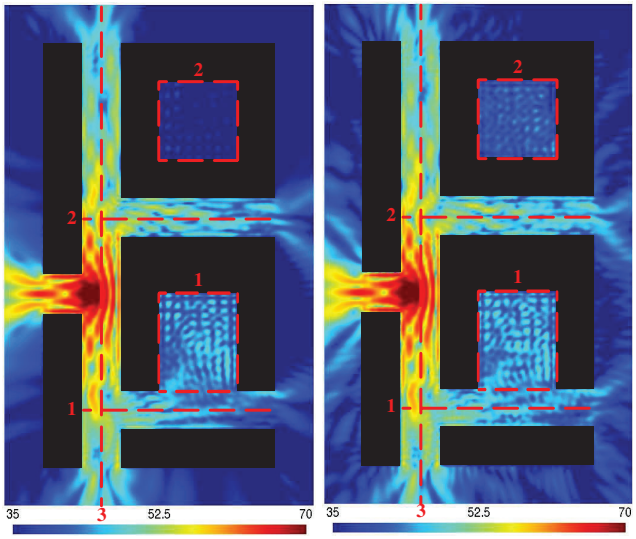

Figure 8: *Sound pressure level in dB(SPL) takes on the receivers' map with the Micado3D software (reference) on the left side and the FMBEM on the right side. The three receivers' lines and the two areas are displayed in red dotted lines.*

Thus the FMBEM provides a substantial benefit regarding the computation time. It is noteworthy that the iterative solver appears to be the most expensive process in terms of computation time as well as for the required memory. We notice that no preconditioning has been used, thus a suitable preconditioner would reduce both computation time and storage memory.

In addition to this general insight, we analyze more precisely the results for two areas belonging to this map. We performed a logarithmic summation on receivers within the red dotted square (cf. figure 8) for the *area 1* and *area 2*. The averaged sound pressure level calculated with *Micado3D* and the FMBEM algorithm is 44.3 against 44.9 dB(SPL) in *area 1* respectively. In the *area 2*, *Micado3D* calculates 33.2 dB(SPL) with a direct solver, 38.2 with an iterative solver, against 40.6 dB(SPL) with the FMBEM algorithm (iterative solver). These results are observed after the stabilization of the convergence of the iterative solver. It points out the fact that the computations in *area 2* are very sensitive. Indeed, the pressure values only depend on the scattering field above the building and neither direct contributions nor reflected are expected.

We also compare, in figure 9, the sound pressure levels along the red dotted lines located in the middle of streets (cf. figure 8). There is a very good agreement on receivers under the influence of a direct contribution coming from the source (figure 9(c)) and a acceptable agreement in the shadows areas (figures 9(a) and 9(b)).

Table 1: *Computing resources related to the main computation stages for both algorithms: Micado3D (BEM variational approach) and FastBEM (collocation approach).*

Method	Direct integrations		Translation matrices		Solver		Total	
	Time(s)	Mem(MB)	Time(s)	Mem(MB)	Time(s)	Mem(MB)	Time(s)	Mem(MB)
BEM (variational)	~ 8000	~ 9000	—	—	~ 21400	—	~ 29400	~ 9000
Fast BEM (collocation)	84	510	136	806	1023	5171	1243	6487

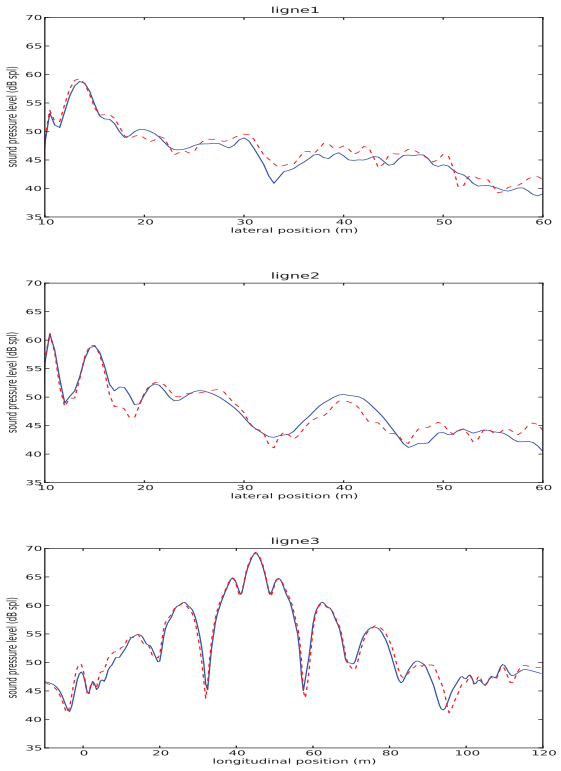

Figure 9: *Sound pressure level in dB(SPL) taken along the 3 red dotted lines with the Micado3D software (reference) in blue lines and the FMBEM in red dotted lines.*

5 Conclusion

As a conclusion, it is clear that the fast multipole method applied with the boundary elements method provides substantial savings regarding the computational time involved and storage memory required specifically for large scale problems, as shown in section (4). However, an iterative solver such as the GMRES can be a possible source of error when compared with direct solvers and must be handle with caution in the more sensitive areas (shadow areas). Because of the very large cost in terms of memory for the storage of Krylov subspaces for a large number of iterations, an appropriate preconditioner seems to be recommended [17]. It also appears that the recursive process for the computation of rotation coefficients in the RCR-decomposition formalism becomes unstable for large expansion orders and it seems that a stable recursion process maybe a purpose of investigation.

References

[1] S. Kirkup. *The boundary element method in acoustics*. Integrated Sound Software, 2007.

[2] L. Greengard and V. Rokhlin. A fast algorithm for particle simulations. *Journal of Comput. Phys.*, (73):325–348, 1987.

[3] N. A. Gumerov and R. Duraiswami. *Fast multipole methods for the Helmholtz equation in three dimensions*. Elsevier, 2004.

[4] S. Chaillat, M. Bonnet, and J. F. Semblat. A multi-level fast multipole bem for 3-d elastodynamics in the frequency domain. *Comput. Method Appl. Mech. Engrg*, (197):4233–4249, 2008.

[5] M. Bonnet, S. Chaillat, and J. F. Semblat. *Multi-level fast multipole BEM for 3D elastodynamics (chapter 2)*. Recent advances in Boundary Elements Methods. Springer edition, 2009.

[6] Y. Liu. *Fast multipoles boundary element method : Theory and applications in engineering*. Cambridge, 2009.

[7] Y. Saad and M. Shultz. Gmres: A generalized minimal residual algorithm for solving non-symmetric linear systems. *SIAM Journal on Scient. and Stat. Comput.*, 7(3), 1986.

[8] N. A. Gumerov and R. Duraiswami. Fast, exact, and stable computation of multipole translation and rotation coefficients for the 3-d helmholtz equation. Technical Report CS-TR-4264, Institute for Advanced Computer Studies, University of Maryland, september 2001.

[9] V. Rokhlin. Diagonal forms of translation operators for the helmholtz equation in three dimensions. *Applied and Computational Harmonic Analysis*, 1:82–93, 1993.

[10] P. N. Swarztrauber and W. F. Spotz. Generalized discrete spherical harmonic transforms. *J. Comput. Phys.*, 159(2):213–230, 2000.

[11] H. Cheng, W. Y. Crutchfield, Z. Gimbutas, L. F. Greengard, J. F. Ethridge, J. Huang, V. Rokhlin, N. Yarvin, and J. Zhao. A wideband fast multipole method for the helmholtz equation in three dimensions. *J. Comput. Phys.*, (216):300–325, 2006.

[12] N. A. Gumerov and R. Duraiswami. A broadband fast multipole accelerated boundary element method for the three dimensional helmholtz equation. *J. Acoust. Soc. Am.*, 125(1):191–205, 2009.

[13] M. Abramowitz and I. A. Stegun. *Handbook of Mathematical Functions*. National Bureau of Standards, Washington, DC, 1964.

[14] S. Li and Q. Huang. A new fast multipole boundary element method for two dimensional acoustic problems. *Comput. Method Appl. Mech. Engrg*, 200:1333–1340, 2011.

[15] M. S. Bapat, L. Shen, and Y. Liu. Adaptive fast multipole boundary element method for three-dimensional half-space acoustic wave problems. *Engineering Analysis with Boundary Elements*, 33:1113–1123, 2009.

[16] P. Jean. A variational approach for the study of outdoor sound propagation and application to railway noise. *Journal of Sound and Vibration*, 212:275–294, 1998.

[17] S. Chaillat, J. F. Semblat, and M. Bonnet. A preconditioned 3-d multi-region fast multipole solver for seismic wave propagation in complex geometries. *Commun. Comput. Phys.*, 11:594–609, 2012.